JACS
JOURNAL OF THE AMERICAN CHEMICAL SOCIETY
Article
pubs.acs.org/JACS

Insights of the Crystallization Process of Molecular Sieve $AlPO_4$-5 Prepared by Solvent-Free Synthesis

Na Sheng,[†] Yueying Chu,[§] Shaohui Xin,[§] Qiang Wang,[§] Xianfeng Yi,[§] Zhaochi Feng,[‡] Xiangju Meng,*[,†] Xiaolong Liu,*[,§] Feng Deng,[§] and Feng-Shou Xiao*[,†,⊥]

[†]Key Lab of Applied Chemistry of Zhejiang Province and Department of Chemistry, Zhejiang University, Hangzhou 310028, China
[§]State Key Laboratory of Magnetic Resonance and Atomic and Molecular Physics, Wuhan Institute of Physics and Mathematics, Chinese Academy of Sciences, Wuhan 430071, China
[‡]State Key Laboratory of Catalysis, Dalian Institute of Chemical Physics, Chinese Academy of Sciences, Dalian 116023, China
[⊥]Key Laboratory of Biomass Chemical Engineering, Ministry of Education, Zhejiang University, Hangzhou 310027, China

Supporting Information

ABSTRACT: Crystallization of $AlPO_4$-5 with AFI structure under solvent-free conditions has been investigated. Attention was mainly focused on the characterization of the intermediate phases formed at the early stages during the crystallization. The development in the long-range ordering of the solid phases as a function of crystallization time was monitored by XRD, SEM, IR, UV-Raman, and MAS NMR techniques. Particularly, the UV-Raman spectroscopy was employed to obtain the information on the formation process of the framework. *J*-HMQC $^{27}Al/^{31}P$ double-resonance NMR experiments were used to identify the P−O−Al bonded species in the intermediate phases. For the first time the P−O−Al bonded species in the intermediate phases can be correctly described through using this advanced NMR technique. The crystallization under solvent-free conditions appears to follow the pathway: The initial amorphous raw material is converted to an intermediate phase which has four-/six-membered ring species, then gradually transformed into crystalline $AlPO_4$-5. This observation is not consistent with the common idea that the intermediate phase is the semicrystalline intermediates with a three-dimensional structure.

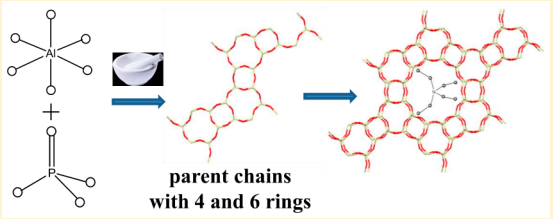

INTRODUCTION

Aluminophosphate ($AlPO_4$-based) molecular sieves and zeolites are widely used in industry for separation and catalysis because of their unique frameworks with specific pores, channels, and cavities at molecular levels.[1,2] Despite tremendous advances in the understanding of the principles underlying the formation of these materials under hydrothermal synthesis (HTS) conditions or dry gel conversion,[3−14] it is an extremely complicated process with multiple reactions and equilibriums occurring simultaneously in solution and solid phases to figure out the crystallization mechanism from the HTS reaction system. Therefore, until now the crystallization mechanisms of molecular sieves are still not understood well on a molecular level, and it is still difficult to design novel framework structures with desirable properties.[15−28]

Through observing the details of the conversion of one-dimensional (1-D) chain to 2-D layer and to 3-D open-framework aluminophosphates, Oliver and co-workers proposed that all the $AlPO_4$-based structures are transformed from a parent single chain with corner-sharing $(Al−O−P)_2$ four-membered rings (4-MRs).[29] No doubt, this observation is very important for understanding the formation process of $AlPO_4$-based molecular sieves. Of course, it is also very important to identify the other small parent units in the structures of the intermediates or precursors. A number of advanced techniques such as UV-Raman,[13,14] SAXS,[30] and X-ray diffraction (XRD)[31] have been taken to study the crystallization processes, and the 1-D growth process and the existence of 4-/6-MR species have been partly confirmed.[13,14,30,31]

Although solid-state NMR techniques have been widely used to characterize the framework of molecular sieves and probe the local environments of the amorphous phases,[32,33] until now no NMR technique has been employed to identify the specific structural units such as 4- and 6-MR in the intermediate phases.

Recently, a number of important zeolites and molecular sieves have been synthesized by our group using solvent-free synthesis methodology. One of the most important benefits of this methodology is providing a simple and uniform reaction system for studying their crystallization process. All of the reactive species are contained in the solid phase, which avoids to distinguishing the reaction intermediates from solution and solids like HTS conditions, which is very favorable for deep understanding the molecular sieve crystallization. Here, we present the investigation on $AlPO_4$-5 crystallization processes under solvent-free conditions. $AlPO_4$-5 is one of the representative $AlPO_4$-based molecular sieves with AFI topology. This material has a wide range of applications as an

Received: February 1, 2016
Published: April 26, 2016

DOI: 10.1021/jacs.6b01200
J. Am. Chem. Soc. 2016, 138, 6171−6176

absorbent or an excellent catalyst support, and now it is considered to be a novel material for optical data storage or other optical applications.[34,35] In this paper, we have characterized the intermediate phases of $AlPO_4$-5, which were obtained by quenching the reaction at different times using several solid-state NMR techniques in combination with powder XRD, SEM, FT-IR, and UV-Raman spectroscopy.

In particular, we have employed ^{27}Al and ^{31}P MAS NMR to probe the development of coordination environments of P and Al atoms. $^{1}H-^{13}C$ CP/MAS NMR is utilized to monitor the development of organic agents (di-*n*-propylamine, DPA; tetraethylammonium, TEA^+) during the crystallization process of $AlPO_4$-5. Besides the routine solid-state NMR techniques have been applied, a specific solid-state NMR technique, the *J*-mediated heteronuclear multiple-quantum correlation (*J*-HMQC) sequence, is taken to characterize the directly boned P−O−Al species, which provides accurate information about the intermediate phases during the framework formation process.

The 2-D INEPT experiment has been successfully applied to reveal the connectivities between AlO_x and PO_4 polyhedra by Fyfe and co-workers,[36a] but its relatively low sensitivity limits deep understanding on the connectivities. Therefore, a new technique in solid-state NMR field-*J*-HMQC sequence is employed in this work to probe the connectivities between spin-1/2 (^{1}H, ^{13}C, ^{31}P, ...) and half-integer quadrupolar (^{11}B, ^{23}Na, ^{17}O, ^{27}Al, ...) nuclei. This PT-*J*-HMQC experiment has been successfully applied to study the structural connectivities of $^{31}P-O-^{27}Al$ on a layered aluminophosphate Mu-4.[36b] In those cases, this method could be used to distinguish the true structural building units from the other reaction intermediates. Obviously, these true structural building units are the keys to find out the real crystallization mechanism of molecular sieves.

EXPERIMENTAL SECTION

Zeolite Synthesis. $AlPO_4$-5 was synthesized under solvent-free condition according to previous works.[37] Typically, the solvent-free synthesis of $AlPO_4$-5 was performed by grinding at room temperature and heating at 200 °C for solid compounds of di-*n*-propylamine phosphate (DPA·H_3PO_4), boehmite, and tetraethylammonium bromide (TEABr) with the molar ratio of Al_2O_3/P_2O_5/DPA/TEABr/H_2O at 1.0/0.8/1.6/0.2/2.4. After dryness at 100 °C, the crystalline product was finally obtained, which was designated as S-APO-5.

Characterization. XRD patterns were measured with a Rigaku Ultimate VI X-ray diffractometer (40 kV, 40 mA) using $Cu_{K\alpha}$ (λ = 1.5406 Å) radiation. Scanning electron microscopy (SEM) experiments were performed on Hitachi SU-1510 and SU-8010 electron microscopes. FT-IR spectra were recorded on Thermo Scientific Nicolet iS5 FT-IR spectrometer. ^{27}Al and ^{31}P solid NMR spectra as well as *J*-HMQC $^{27}Al/^{31}P$ double-resonance NMR experiments were recorded on a Bruker Infinity Plus 500 spectrometer, and the chemical shifts were referenced to $Al(H_2O)_6^{3+}$ (1 M, 0 ppm). All the liquid NMR experiments were performed on a Bruker 600 spectrometer at resonance frequencies of 600.13 and 150.92 MHz for ^{1}H and ^{13}C, respectively. ^{1}H NMR spectra were recorded with a pulse width of 9.8 μs and a recycle delay of 2 s. A 30° exiting pulse with 2 s repetition time was used for ^{13}C NMR experiments. The chemical shifts were externally referenced to TMS. UV-Raman spectra were recorded on a Jobin-Yvon T64000 triple-stage spectrograph with spectral resolution of 2 cm^{-1}. The 266 nm line from the double frequency of Coherent Verdi-V10 laser through Wave Train CW frequency doubler was used as another excitation source. The power of the 266 nm line at samples was below 1.0 mW.

RESULTS AND DISCUSSION

Figure S1A shows XRD patterns of the washed samples with different crystallization time, which indicate the crystalline evolution of the solid mixtures. For the initial samples (Figure S1A-a), the XRD pattern shows only the peaks from DPA·H_3PO_4.[37] As heating to 1.0 h (Figure S1A-b), two broad humps between 12.5° and 30° appear; when heating to 1.5 h (Figure S1A-c), three weak diffraction peaks between 19° and 22.5° are shown, which suggest that the periodic framework of crystalline $AlPO_4$-5 starts to be formed from an amorphous phase. Heating to 2 h (Figure S1A-d) leads to the formation of the fingerprint peaks associated with the AFI-type framework at 7.5°, 19.9°, 21.1°, and 22.6°. With increasing the time to 3 h (Figure S1A-e), nearly 80% raw materials are transformed into crystalline molecular sieves of $AlPO_4$-5 (Figure S1B). The fully crystalline molecular sieve is obtained when the reaction time is over 4 h (Figure S1A-f,g). Compared with HTS, the solvent-free synthesis takes shorter reaction time, therefore saving energy; meanwhile, the yield under solvent-free synthesis is much higher than that of HTS due to no loss of nutrients in the solvent.[32b,37]

Figure S2 shows IR spectra of the washed samples with different crystallization time for understanding the reactive intermediates. Before heating (Figure S2a,b), the sample shows only the peaks from DPA·H_3PO_4.[37] After heating for 1 h (Figure S2c), several weak bands in the range of 2600−3000 cm^{-1} are assigned to C−H stretching modes of the template molecules. The bands at 1470 and 1400 cm^{-1} are considered to be associated with the bending modes of the $-CH_2$ and $-CH_3$ groups of the TEA cations.[38] The strong band at 1123 cm^{-1} is characteristic of the asymmetric stretching vibration of the Al−O−P units in the amorphous phase.[39,40] With increasing the crystallization time from 1.5 to 24 h (Figure S2d−h), several weak bands at 499, 627, 739, 889, and 1216 cm^{-1} appear, which are related to the symmetric and asymmetric stretching vibrations of the Al−O−P units, and the band appearing at 550 cm^{-1} arises from the P−O or Al−O bending modes.[40] All above observations suggest that the P−O−Al units and the TEABr molecules exist in the amorphous phase. The two strong bands at 3422 and 1645 cm^{-1} in the IR spectra correspond to the specificity of water molecules adsorbed on OH groups and bending vibrations of these surface-adsorbed water molecules.[32b,41]

Figure S3 shows the SEM images of the washed samples at different crystallization time. With increasing time, the amorphous phase has gradually transformed into crystal morphology. Notably, after heating for 1.5 h (Figure S3c), it is observed the crystalline phase; after 24 h heating (Figure S3f), the solids are fully crystallized. The crystalline growth informed from the SEM images are well consistent with those observed from XRD patterns.

The Raman spectra in the T−O−T (T = tetrahedral site) bending region are very sensitive to the ring systems existing in the molecular sieve frameworks.[42] In order to make sure that the characteristic 12-membered ring (12-MR) channels have been formed, UV-Raman experiments have been taken for selected washed samples in Figure 1. For $AlPO_4$-5, its 12-MR channel has a characteristic ring breathing mode at 260 cm^{-1}.[14,42a] The starting solid mixture exhibits two well-resolved signals at 310 and 412 cm^{-1} in the Raman spectrum (Figure 1a), which is associated with those of the Raman spectrum of DPA·H_3PO_4 molecule (Figure S4a). After heating for 1 h

DOI: 10.1021/jacs.6b01200
J. Am. Chem. Soc. 2016, 138, 6171−6176

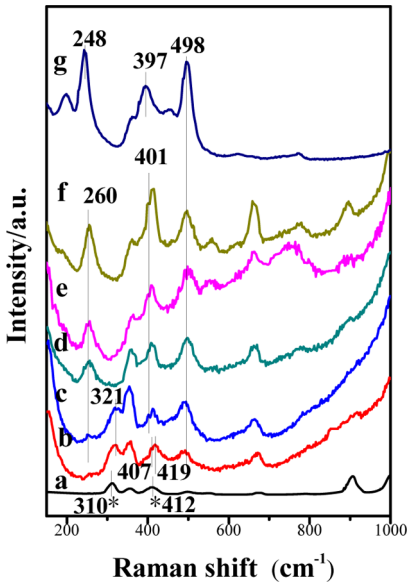

Figure 1. Raman spectra of the samples synthesized at different crystallization time (a) 0, (b) 1, (c) 1.5, (d) 2, (e) 3, and (f) 24 h and (g) the calcined sample of 24 h.

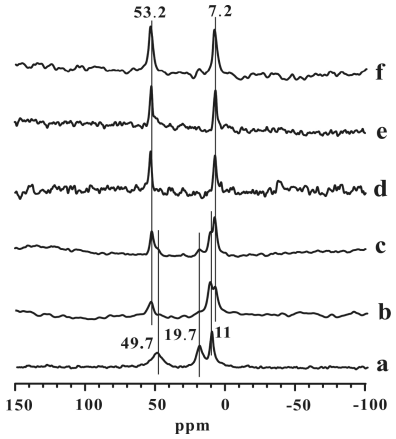

Figure 2. $^{1}H-^{13}C$ CP/MAS NMR spectra of the samples synthesized at different crystallization time of (a) 0, (b) 1, (c) 1.5, (d) 2, (e) 3, and (f) 24 h.

(Figure 1b), the sample shows the bands at 321, 407, 419, and 498 cm^{-1}. The bands at 321 and 419 cm^{-1} are shifted from the bands at 310 and 412 cm^{-1}, which is due to the interaction between the DPA·H_3PO_4 molecule with aluminum species. The Raman bands at 407 and 498 cm^{-1} assigned to be the distortive 6-MRs and normal 4-MRs appear in the very early stages of the synthesis, participating in the formation of channel-like structures.[14,29,42] When increasing the time to 1.5 h (Figure 1c), a weak band with a maximum at 260 cm^{-1} starts to be observed, which means the semicrystalline intermediate structures with 12-MR are formed. At the same time, the band at 401 cm^{-1} shifted from the band at 407 cm^{-1} in Figure 1b becomes stronger, which suggests that more 6-MRs are formed. Continuing to increase the crystallization time from 2 to 24 h (Figure 1d,f), the intensities of Raman bands at 260, 401, and 498 cm^{-1} gradually increase, suggesting that the 12-MR crystalline structures are well constructed through arrangements of the 6- and 4-MRs. After calcination of the sample crystallized at 24 h (Figure 1g), the sample clearly shows the band at 397 cm^{-1} assigned to 6-MRs. In addition, to remove the UV-Raman signals associated with DPA·H_3PO_4 in the synthesis, we have compared as-synthesized, washed, and calcined samples, as shown in Figure S4. Obviously, the Raman bands at 260, 401, and 498 cm^{-1} should be confirmed to associate with 12-, 6-, and 4-MR structure.

To investigate the roles of TEABr and DPA molecules during the crystallization process, $^{1}H-^{13}C$ NMR spectra were performed. Figure 2 shows $^{1}H-^{13}C$ CP/MAS NMR spectra of the washed samples prepared at different synthesis time. Three strong DPA·H_3PO_4 signals are dominant in the spectrum of the initial sample (Figure 2a), in which raw materials are just mixed without heating. The reason is that the mole amount of DPA is far more than that of TEABr in the raw material. After heating for 1 h (Figure 2b), two signals at 53.2 and 7.2 ppm assigned to the methylene and methyl groups of TEABr appear, indicating that the TEA cations are similar to the role of the structural directing agent, interacting with the inorganic species even if the solids are still amorphous in nature.[32b] After heating for 1.5 h (Figure 2c), the signals from DPA are significantly reduced, which might be related to the fact that most of DPA·H_3PO_4 molecules in the system are dissociated to DPA and H_3PO_4. At the same time, the produced H_3PO_4 at high temperature might react with Al_2O_3 to form $(Al-O-P)_n$ species. Possibly, the DPA·H_3PO_4 complexes made the crystallization time shorter than that of traditional hydrothermal synthesis and produced a uniform crystallized molecular sieves. They can be a good candidate of phosphorus sources. The reaction equation is proposed as follows:

$$\frac{n}{2}Al_2O_3 + \frac{n}{2}DPA{\cdot}H_3PO_4 \rightarrow (Al-O-P)_n + nDPA$$

As observed in Figure 2, the $^{1}H-^{13}C$ NMR spectra demonstrate that the relative intensities of DPA molecules are gradually decreased and TEA^+ species are gradually increased with prolonging the crystallization time in the samples. In the pure $AlPO_4$-5 product we cannot observe the DPA molecules, which means that the DPA molecules do not act as pore filling agents or structure-directing agents in the synthesis, but TEA^+ species do.

Figure S5 shows ^{1}H and ^{13}C liquid NMR spectra of a filtrate obtained from the fully crystallized sample, showing peaks at 0.7, 1.4, 2.7 ppm in ^{1}H spectrum and 10, 19, 49 ppm in ^{13}C spectrum, which are assigned to characteristic of DPA species. These results confirm the direct decomposition of DPA·H_3PO_4 to DPA and H_3PO_4, rather than templation of $AlPO_4$-5 molecular sieve. Figure S6 shows TG-DTA curve of DPA·H_3PO_4, giving that the DPA·H_3PO_4 starts to decompose from about 160 °C. This observation strongly supports our suggestion that the DPA·H_3PO_4 molecules are dissociated to DPA and H_3PO_4 under solvent-free conditions (reaction temperature at 200 °C). In fact, the DPA·H_3PO_4 molecules provide a solid P source for the solvent-free synthesis of $AlPO_4$-5.

Figure 3A shows ^{27}Al MAS NMR spectra of the samples synthesized at different crystallization time. For the starting raw solid mixtures (Figure 3A-a), only a strong signal at 8.3 ppm is observed, which is correspondent to boehmite. After heating for 1 h (Figure 3A-b), ^{27}Al spectrum of the sample shows a weak signal at 42.6 ppm and a strong signal at 8.3 ppm. Previous work has assigned that the weak signal is from the tetrahedral Al connected with phosphate $[Al(OP)_4]$, while the strong

DOI: 10.1021/jacs.6b01200
J. Am. Chem. Soc. 2016, 138, 6171−6176

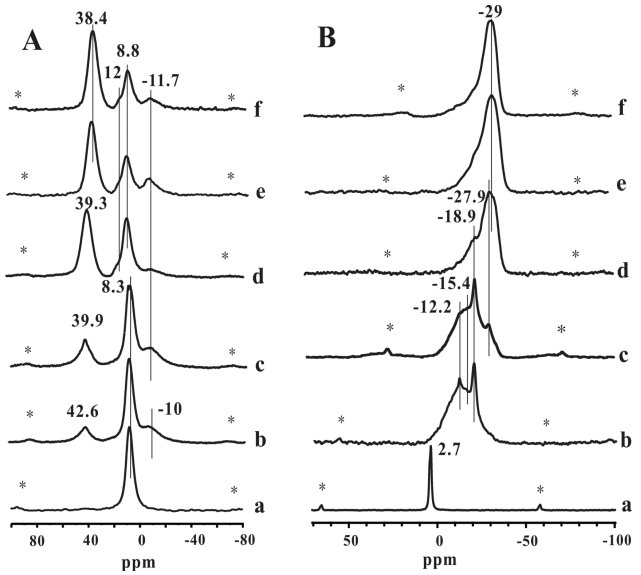

Figure 3. (A) ^{27}Al and (B) ^{31}P MAS NMR spectra of the samples synthesized at different crystallization time of (a) 0, (b) 1, (c) 1.5, (d) 2, (e) 3, and (f) 24 h.

signal is related to unreacted boehmite in aluminophosphates.[32b,38]

The ^{27}Al spectrum of the 1.5 h (Figure 3A-c) heated solid shows a similar feature to the 1 h heated solid. After heating the mixtures for 2 h (Figure 3A-d), the intensity of the tetrahedral Al signals at 42.6 ppm is increased, and the "octahedral" Al signals are decreased, suggesting that the solids get more organized. Further heating does not really change the relative intensities of the signals, which means almost all raw materials have been transformed to crystalline products after heating for 3 h (Figure 3A-e). It is also observed that the chemical shift of the tetrahedral Al changes from 42.6 to 38.4 ppm during the crystallization, which suggests the chemical environment of Al atoms between the amorphous and crystalline phase are slightly different. The very weak peak at −11.7 ppm in Figure 3A can be attributed to the extra-frame octahedral Al.[32b,37,43−45]

Figure 3B shows ^{31}P MAS NMR spectra of the samples synthesized at different crystallization time. For the initial raw mixtures (Figure 3B-a), only one strong signal at 2.7 ppm associated with DPA·H_3PO_4 is observed.

The ^{13}P spectrum of the 1 h (Figure 3B-b) heated mixture shows a broad signal from −12.2 to −15.4 ppm and a sharp signal at −18.9 ppm, indicating the presence of several kinds of P−O−Al units in the mixture.[32c,46] Particularly, the sharp ^{31}P peak at −18.9 ppm has been assigned to $P(OAl)_3(=O)$ and/or $P(OAl)_3(-OH)$ species.[43,47,48] The ^{31}P spectrum of the 1.5 h (Figure 3B-c) heated sample gives the signal at −27.9 ppm, which is assigned to $P(OAl)_4$.[3,37,45] Simultaneously, the signal intensities (−12.2 to −15.4 ppm) become weaker. As heating time to 3 h (Figure 3B-e), there is only signal around −29 ppm assigned to the tetrahedral P in the $AlPO_4$-5 crystalline framework, indicating its full crystallization.

For 1D ^{31}P and ^{27}Al NMR spectra, it has a great challenge to get high-resolution NMR spectra of the aluminophosphate intermediate species because their signals are highly overlapped. To deeply understand the crystallization process and the aluminophosphate structures in the intermediates, ^{31}P-{^{27}Al} *J*-HMQC experiments have been performed, which can provide the bonded P−O−Al structural information. In contrast, HETCOR method only provides the spatial information. Obviously, the *J*- HMQC experiments can be used to identify the complex species existing in the crystallization of molecular sieves.

In the spectrum of the initial sample, there is no correlated signal (Figure 4A) because no Al−O−P units are in the raw mixtures. For crystallization with 1 h (Figure 4B), the top cross contours relate the signals of P atoms with chemical shift from −12.2 ppm to −15.4 ppm with the signals from Al with

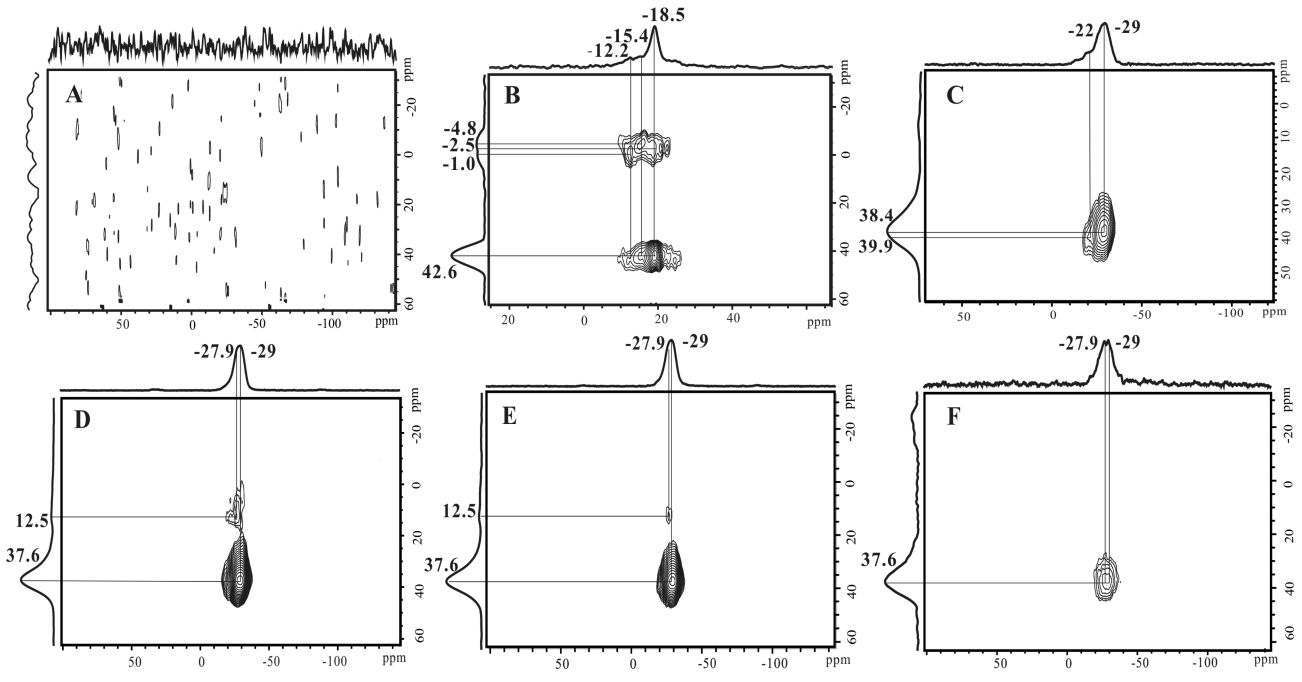

Figure 4. ^{31}P-{^{27}Al} *J*-HMQC spectra of washed samples synthesized at crystallization time of (A) 0, (B) 1, (C) 1.5, (D) 3, (E) 24 h, and (F) 24 h calcined.

DOI: 10.1021/jacs.6b01200
J. Am. Chem. Soc. 2016, 138, 6171−6176

chemical shift at −4.8 and −1.0 ppm, these correlated peaks are thought to be the linear tetrahedral Al and P units [(P−O−Al)$_n$] in the intermediates.[49]

The top cross contours in Figure 4B mainly relate the signals of P atoms with chemical shift at −18.5 ppm with the signals from Al with the shift from −4.8 to −1.0 ppm; these correlated peaks were considered to be the tetrahedral Al and P units that are formed to 4-/6-MRs and branched ring units in the intermediates. The UV-Raman spectra of the sample support the presence of 4-/6-MRs in the system (Figure 1). These 4-/6-MRs could be the dominant Al−O−P bonded species due to their relatively strong signals. The 4-/6-MRs will be organized by the association of TEABr molecules and form the 1D Al_2P_2 parent chains and 3D frameworks around the TEABr molecules. We believe that this stage is the true nucleation stage for assembling the AFI framework. Later observations prove that this stage is the key for the intermediate phase to be further crystallized because the ring species provide the basic construction materials for building a 3-D framework.[50]

When the heating time is increased to 1.5 h (Figure 4C), the cross contour shows that all Al atoms and P atoms are in the framework of $AlPO_4$-5. Even if XRD pattern of the sample does not show characteristic peaks related to $AlPO_4$-5, the 2D NMR spectrum clearly demonstrates that the sample synthesized at 1.5 h is well crystallized. It is worth mentioning that the Al−O−P species with P chemical shift −18.5 ppm are almost totally consumed, but 1D ^{31}P MAS spectrum does not show this transformation. This observation also supports that the ring species are the nutrients and building blocks for the formation of aluminophosphate-based molecular sieve $AlPO_4$-5. Longer crystallization time just makes the crystals more perfect and grow bigger. In Figure 4D,E, the cross contour with Al signal at 12.5 ppm can be assigned to the penta-coordinate Al.[37] For calcined sample (Figure 4F), this contour disappears for losing water molecules. Clearly, the 2D NMR technique could be a new tool to investigate the complex intermediates in the crystallization of aluminophosphate molecular sieves.

Theoretical simulation of ^{31}P and ^{27}Al chemical shifts can been applied to provide further evidence on the assignments of the intermediates.[51] Compared with the 4-MR chain (Figure S7) and the 6-MR chain (Figure S8), the theoretically simulated ^{27}Al (2.8 to −7.0 ppm) and ^{31}P NMR (−16.3 to −17.0 ppm) for 4-/6MR chain (Figure 5) are very close to the

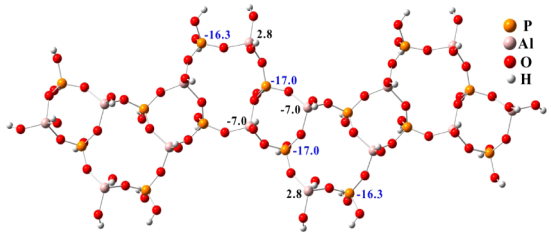

Figure 5. Optimized 4-/6-MR chain structure. The simulated ^{31}P (blue) and ^{27}Al (black) NMR labeled in ppm.

experimental results (−4.8 to −1.0 ppm for ^{27}Al and −18.5 ppm for ^{31}P), which strongly supports the experimental results that the 4-/6-MR chains as the intermediates assemble to 1D chains and 3D framework.

On the basis of above experimental results, the crystallization process of the $AlPO_4$-5 is proposed in Scheme 1. The initial amorphous raw material is converted to an intermediate phase with 4-/6-MR species, then gradually transformed into crystalline $AlPO_4$-5.

Scheme 1. Illustration of Possible Formation for Solvent-Free Synthesis of $AlPO_4$-5

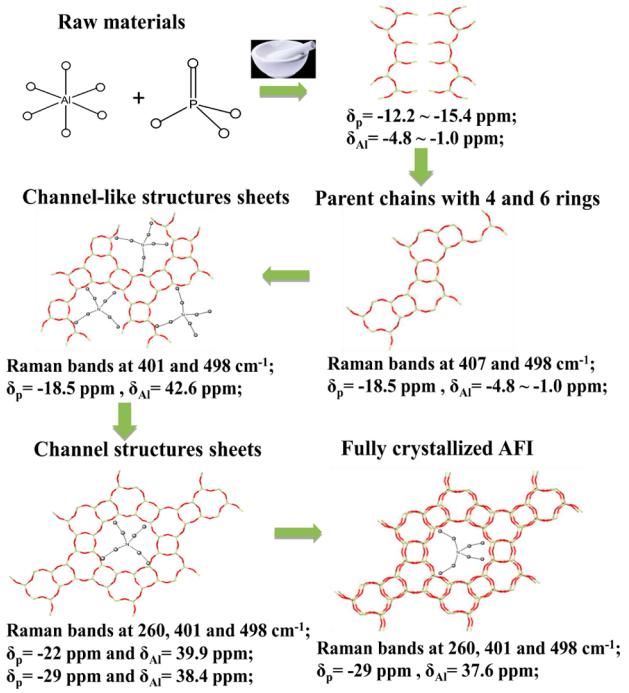

CONCLUSIONS

We have investigated the formation process of molecular sieve $AlPO_4$-5 as a function of crystallization time under solvent-free conditions. This process follows a self-assembly mechanism, involving the formation of a key intermediate consisting of 4-/6-MR chains, which is not detectable by XRD pattern, but *J*-HMQC ^{31}P/^{27}Al technique clearly observes this key stage. This intermediate provides the basic building blocks for further forming the target $AlPO_4$-5 crystals.

ASSOCIATED CONTENT

Supporting Information

The Supporting Information is available free of charge on the ACS Publications website at DOI: 10.1021/jacs.6b01200.

Characterization details (PDF)

AUTHOR INFORMATION

Corresponding Authors

*mengxj@zju.edu.cn
*xiaolong.liu@wipm.ac.cn
*fsxiao@zju.edu.cn

Notes

The authors declare no competing financial interest.

ACKNOWLEDGMENTS

This work was supported by the National Natural Science Foundation of China (21333009, 21422306, 91545111, and 21303253), Zhejiang Provincial Natural Science Foundation of China under grant no. LR15B030001, and the Fundamental

DOI: 10.1021/jacs.6b01200
J. Am. Chem. Soc. 2016, 138, 6171−6176

Research Funds for the Central Universities (2015XZZX004-04).

REFERENCES

(1) Davis, M. E. *Nature* **2002**, *417*, 813−821.
(2) Jin, Y. Y.; Sun, Q.; Qi, G. D.; Yang, C. G.; Xu, J.; Chen, F.; Meng, X. J.; Deng, F.; Xiao, F.-S. *Angew. Chem., Int. Ed.* **2013**, *52*, 9172−9175.
(3) (a) Chen, B. H.; Huang, Y. N. *J. Am. Chem. Soc.* **2006**, *128*, 6437−6446. (b) Fyfe, C. A.; Bretherton, J. L.; Lam, L. Y. *J. Am. Chem. Soc.* **2001**, *123*, 5285−5291.
(4) Cai, R.; Liu, Y.; Gu, S.; Yan, Y. S. *J. Am. Chem. Soc.* **2010**, *132*, 12776−12777.
(5) Li, J. Z.; Wei, Y. X.; Chen, J. R.; Tian, P.; Su, X.; Qi, Y.; Wang, Q. Y.; Zhou, Y.; He, Y. L.; Liu, Z. M. *J. Am. Chem. Soc.* **2012**, *134*, 836−839.
(6) Park, M. B.; Cho, S. J.; Hong, S. B. *J. Am. Chem. Soc.* **2011**, *133*, 1917−1934.
(7) Park, M. B.; Lee, Y.; Zheng, A.; Xiao, F.-S.; Nicholas, C. P.; Lewis, G. J.; Hong, S. B. *J. Am. Chem. Soc.* **2013**, *135*, 2248−2255.
(8) Kumar, M.; Luo, H.; Roman-Leshkov, Y.; Rimer, J. D. *J. Am. Chem. Soc.* **2015**, *137*, 13007−13017.
(9) Lupulescu, A. I.; Rimer, J. D. *Science* **2014**, *344*, 729−732.
(10) Lupulescu, A. I.; Kumar, M.; Rimer, J. D. *J. Am. Chem. Soc.* **2013**, *135*, 6608−6617.
(11) Chen, H. Y.; Wydra, J.; Zhang, X. Y.; Lee, P. S.; Wang, Z. P.; Fan, W.; Tsapatsis, M. *J. Am. Chem. Soc.* **2011**, *133*, 12390−12393.
(12) Ikuno, T.; Chaikittisilp, W.; Liu, Z. D.; Iida, T.; Yanaba, Y.; Yoshikawa, T.; Kohara, S.; Wakihara, T.; Okubo, T. *J. Am. Chem. Soc.* **2015**, *137*, 14533−14544.
(13) O'Brien, M. G.; Beale, A. M.; Catlow, C. R. A.; Weckhuysen, B. M. *J. Am. Chem. Soc.* **2006**, *128*, 11744−11745.
(14) Fan, F. T.; Feng, Z. C.; Sun, K. J.; Guo, M. L.; Guo, Q.; Song, Y.; Li, W. X.; Li, C. *Angew. Chem., Int. Ed.* **2009**, *48*, 8743−8747.
(15) Davis, T. M.; Drews, T. O.; Ramanan, H.; He, C.; Dong, J.; Schnablegger, H.; Katsoulakis, M. A.; Kokkoli, E.; McCormick, A. V.; Penn, R. L.; Tsapatsis, M. *Nat. Mater.* **2006**, *5*, 400−408.
(16) Alabarse, F. G.; Rouquette, J.; Coasne, B.; Haidoux, A.; Paulmann, C.; Cambon, O.; Haines, J. *J. Am. Chem. Soc.* **2015**, *137*, 584−587.
(17) Zones, S. I.; Benin, A.; Hwang, S. J.; Xie, D.; Elomari, S.; Hsieh, M. *J. Am. Chem. Soc.* **2014**, *136*, 1462−1471.
(18) Ren, L. M.; Li, C.; Fan, F. T.; Feng, Z. C.; Xiao, F.-S. *Chem. - Eur. J.* **2011**, *17*, 6162−6169.
(19) Yu, J. H.; Xu, R. R. *Chem. Soc. Rev.* **2006**, *35*, 593−604.
(20) Shayib, R. M.; George, N. C.; Seshadri, R.; Burton, A. W.; Zones, S. I.; Chmelka, B. F. *J. Am. Chem. Soc.* **2011**, *133*, 18728−18741.
(21) Huo, H.; Peng, L. M.; Gan, Z. H.; Grey, C. P. *J. Am. Chem. Soc.* **2012**, *134*, 9708−9720.
(22) Kim, M.; Li, H.; Davis, M. E. *Microporous Mater.* **1993**, *1*, 191−200.
(23) Rao, P. R. H. P.; Matsukata, M. *Chem. Commun.* **1996**, 1441−1442.
(24) Valtchev, V. P.; Bozhilov, K. N. *J. Am. Chem. Soc.* **2005**, *127*, 16171−16177.
(25) Moliner, M.; Martinez, C.; Corma, A. *Chem. Mater.* **2014**, *26*, 246−258.
(26) Moliner, M.; Rey, F.; Corma, A. *Angew. Chem., Int. Ed.* **2013**, *52*, 13880−13889.
(27) Seo, Y.; Lee, S.; Jo, C.; Ryoo, R. *J. Am. Chem. Soc.* **2013**, *135*, 8806−8809.
(28) Itani, L.; Liu, Y.; Zhang, W.; Bozhilov, K. N.; Delmotte, L.; Valtchev, V. *J. Am. Chem. Soc.* **2009**, *131*, 10127−10139.
(29) (a) Oliver, S.; Kuperman, A.; Lough, A.; Ozin, G. A. *Chem. Mater.* **1996**, *8*, 2391−2398. (b) Oliver, S.; Kuperman, A.; Ozin, G. A. *Angew. Chem., Int. Ed.* **1998**, *37*, 46−62.
(30) (a) de Moor, P.-P. E. A.; Beelen, T. P. M.; van Santen, R. A.; Tsuji, K.; Davis, M. E. *Chem. Mater.* **1999**, *11*, 36−43. (b) Fan, W.; Ogura, M.; Sankar, G.; Okubo, T. *Chem. Mater.* **2007**, *19*, 1906−1917.
(31) Rey, F.; Sankar, G.; Thomas, J. M.; Barrett, P. A.; Lewis, D. W.; Catlow, C. R. A.; Clark, S. M.; Greaves, G. N. *Chem. Mater.* **1995**, *7*, 1435−1436.
(32) (a) Huang, Y. N.; Machado, D.; Kirby, C. W. *J. Phys. Chem. B* **2004**, *108*, 1855−1865. (b) Xu, J.; Chen, L.; Zeng, D.; Yang, J.; Zhang, M.; Ye, C.; Deng, F. *J. Phys. Chem. B* **2007**, *111*, 7105−7113. (c) Chen, B. H.; Huang, Y. N. *J. Phys. Chem. C* **2007**, *111*, 15236−15243.
(33) Deeg, F. W.; Ehrl, M.; Hoppe, R.; Schulz-Ekloff, G.; Wöhrle, D. *J. Lumin.* **1992**, *53*, 219−222.
(34) Caro, J.; Finger, G.; Kornatowski, J.; Richter-Mendau, J.; Werner, L.; Zibrowius, B. *Adv. Mater.* **1992**, *4*, 273−276.
(35) (a) Merle, N.; Trebosc, J.; Baudouin, A.; Del Rosal, I.; Maron, L.; Szeto, K.; Genelot, M.; Mortreux, A.; Taoufik, M.; Delevoye, L.; Gauvin, R. M. *J. Am. Chem. Soc.* **2012**, *134*, 9263−9275. (b) Mazoyer, E.; Trebosc, J.; Baudouin, A.; Boyron, O.; Pelletier, J.; Basset, J. M.; Vitorino, M. J.; Nicholas, C. P.; Gauvin, R. M.; Taoufik, M.; Delevoye, L. *Angew. Chem., Int. Ed.* **2010**, *49*, 9854−9858.
(36) (a) Fyfe, C. A.; Meyer zu Altenschildesche, H.; Wong-Moon, K. C.; Grondey, H.; Chezeau, J. M. *Solid State Nucl. Magn. Reson.* **1997**, *9*, 97−106. (b) Wang, Q.; Trebosc, J.; Li, Y. X.; Xu, J.; Hu, B. W.; Feng, N. D.; Chen, Q.; Lafon, O.; Amoureux, J. P.; Deng, F. *Chem. Commun.* **2013**, *49*, 6653−6655.
(37) Jin, Y. Y.; Chen, X.; Sun, Q.; Sheng, N.; Liu, Y.; Bian, C. Q.; Chen, F.; Meng, X. J.; Xiao, F.-S. *Chem. - Eur. J.* **2014**, *20*, 17616−17623.
(38) Popescu, S. C.; Thomson, S.; Howe, R. F. *Phys. Chem. Chem. Phys.* **2001**, *3*, 111−118.
(39) Wilson, S. T. *Stud. Surf. Sci. Catal.* **1991**, *58*, 137−151.
(40) Davis, M. E.; Montes, C.; Hathaway, P. E.; Arhancet, J. P.; Hasha, D. L.; Garces, J. M. *J. Am. Chem. Soc.* **1989**, *111*, 3919−3924.
(41) Ren, T. Z.; Yuan, Z. Y.; Su, B. L. *Chem. Phys. Lett.* **2003**, *374*, 170−175.
(42) (a) Holmes, A. J.; Kirkby, S. J.; Ozin, G. A.; Young, D. *J. Phys. Chem.* **1994**, *98*, 4677−4682. (b) Dutta, P. K.; Twu, J. *J. Phys. Chem.* **1991**, *95*, 2498−2501. (c) Konidakis, I.; Varsamis, C. E.; Kamitsos, E. I.; Möncke, D.; Ehrt, D. *J. Phys. Chem. C* **2010**, *114*, 9125−9138.
(43) (a) Sayari, A.; Moudrakovski, I.; Reddy, J. S.; Ratcliffe, C. I.; Ripmeester, J. A.; Preston, K. F. *Chem. Mater.* **1996**, *8*, 2080−2088. (b) Hasha, D.; Saldarriaga, L. S. d.; Saldarriaga, C.; Hathaway, P. E.; Cox, D. F.; Davis, M. E. *J. Am. Chem. Soc.* **1988**, *110*, 2127−2135.
(44) Blackwell, C. S.; Patton, R. L. *J. Phys. Chem.* **1988**, *92*, 3965−3970.
(45) Xi, D. Y.; Sun, Q. M.; Xu, J.; Cho, M. H.; Cho, H. S.; Asahina, S.; Li, Y.; Deng, F.; Terasaki, O.; Yu, J. H. *J. Mater. Chem. A* **2014**, *2*, 17994−18004.
(46) Hartmann, P.; Vogel, J.; Schnabel, B. *J. Magn. Reson., Ser. A* **1994**, *111*, 110−114.
(47) (a) Khimyak, Y. Z.; Kinowski, J. *J. Chem. Soc., Faraday Trans.* **1998**, *94*, 2241−2247. (b) Tuel, A.; Gramlich, V.; Baerlocher, Ch. *Microporous Mesoporous Mater.* **2001**, *46*, 57−66.
(48) Chen, B. H.; Kirby, C. W.; Huang, Y. N. *J. Phys. Chem. C* **2009**, *113*, 15868−15876.
(49) Tian, P.; Su, X.; Wang, Y. X.; Xia, Q. H.; Zhang, Y.; Fan, D.; Meng, S. H.; Liu, Z. M. *Chem. Mater.* **2011**, *23*, 1406−1413.
(50) Maldonado, M.; Oleksiak, M. D.; Chinta, S.; Rimer, J. D. *J. Am. Chem. Soc.* **2013**, *135*, 2641−2652.
(51) (a) Zheng, A. M.; Han, B.; Li, B. J.; Liu, S. B.; Deng, F. *Chem. Commun.* **2012**, *48*, 6936−6938. (b) Zheng, A. M.; Han, B.; Li, B. J.; Liu, S. B.; Deng, F. *J. Phys. Chem. C* **2009**, *113*, 15018−15023.

DOI: 10.1021/jacs.6b01200
J. Am. Chem. Soc. 2016, 138, 6171−6176